Dye exclusion microfluidic microscopy

Ethan Schonbrun,* Giuseppe Di Caprio, and Diane Schaak

Rowland Institute at Harvard, Harvard University, Cambridge, Massachusetts 02142, USA
**schonbrun@rowland.harvard.edu*

Abstract: We present an optical system to measure height maps of non-adherent cells as they flow through a microfluidic channel. The cells are suspended in an index-matching absorbing buffer, where cell height is evaluated by measuring the difference in absorption between the cell and the background. Unlike interferometric microscopes, the measured cell height is nearly independent of the cell's optical properties. The height maps are captured using a single exposure of a color camera, and consequently the system is capable of high-throughput characterization of large collections of cells. Using this system, we have measured more than 1600 height maps and volumes of three different leukemia cell lines.

OCIS Codes: (170.1530) Cell analysis; (110.0180) Microscopy; (090.1995) Digital holography.

References and links

1. A. Tzur, J. K. Moore, P. Jorgensen, H. M. Shapiro, and M. W. Kirschner, "Optimizing optical flow cytometry for cell volume-based sorting and analysis," PLoS ONE **6**(1), e16053 (2011).
2. M. Wendel, L. Bazhenova, R. Boshuizen, A. Kolatkar, M. Honnatti, E. H. Cho, D. Marrinucci, A. Sandhu, A. Perricone, P. Thistlethwaite, K. Bethel, J. Nieva, M. van den Heuvel, and P. Kuhn, "Fluid biopsy for circulating tumor cell identification in patients with early-and late-stage non-small cell lung cancer: a glimpse into lung cancer biology," Phys. Biol. **9**(1), 016005 (2012).
3. T. R. Jones, A. E. Carpenter, M. R. Lamprecht, J. Moffat, S. J. Silver, J. K. Grenier, A. B. Castoreno, U. S. Eggert, D. E. Root, P. Golland, and D. M. Sabatini, "Scoring diverse cellular morphologies in image-based screens with iterative feedback and machine learning," Proc. Natl. Acad. Sci. U.S.A. **106**(6), 1826–1831 (2009).
4. D. A. Basiji, W. E. Ortyn, L. Liang, V. Venkatachalam, and P. Morrissey, "Cellular image analysis and imaging by flow cytometry," Clin. Lab. Med. **27**(3), 653–670, viii (2007).
5. E. Schonbrun, S. S. Gorthi, and D. Schaak, "Microfabricated multiple field of view imaging flow cytometry," Lab Chip **12**(2), 268–273 (2011).
6. J. M. Higgins and L. Mahadevan, "Physiological and pathological population dynamics of circulating human red blood cells," Proc. Natl. Acad. Sci. U.S.A. **107**(47), 20587–20592 (2010).
7. S. Son, A. Tzur, Y. Weng, P. Jorgensen, J. Kim, M. W. Kirschner, and S. R. Manalis, "Direct observation of mammalian cell growth and size regulation," Nat. Methods **9**(9), 910–912 (2012).
8. B. Rappaz, A. Barbul, Y. Emery, R. Korenstein, C. Depeursinge, P. J. Magistretti, and P. Marquet, "Comparative study of human erythrocytes by digital holographic microscopy, confocal microscopy, and impedance volume analyzer," Cytometry A **73A**(10), 895–903 (2008).
9. G. Popescu, T. Ikeda, R. R. Dasari, and M. S. Feld, "Diffraction phase microscopy for quantifying cell structure and dynamics," Opt. Lett. **31**(6), 775–777 (2006).
10. B. Kemper and G. von Bally, "Digital holographic microscopy for live cell applications and technical inspection," Appl. Opt. **47**(4), A52–A61 (2008).
11. G. Di Caprio, M. A. Gioffre, N. Saffioti, S. Grilli, P. Ferraro, R. Puglisi, D. Balduzzi, A. Galli, and G. Coppola, "Quantitative label-free animal sperm imaging by means of digital holographic microscopy," IEEE J. Sel. Top. Quantum Electron. **16**(4), 833–840 (2010).
12. A. Greenbaum, W. Luo, T. W. Su, Z. Göröcs, L. Xue, S. O. Isikman, A. F. Coskun, O. Mudanyali, and A. Ozcan, "Imaging without lenses: achievements and remaining challenges of wide-field on-chip microscopy," Nat. Methods **9**(9), 889–895 (2012).
13. S. S. Gorthi and E. Schonbrun, "Phase imaging flow cytometry using a focus-stack collecting microscope," Opt. Lett. **37**(4), 707–709 (2012).
14. W. Choi, C. Fang-Yen, K. Badizadegan, S. Oh, N. Lue, R. R. Dasari, and M. S. Feld, "Tomographic phase microscopy," Nat. Methods **4**(9), 717–719 (2007).
15. M. L. Gray, R. A. Hoffman, and W. P. Hansen, "A new method for cell volume measurement based on volume exclusion of a fluorescent dye," Cytometry **3**(6), 428–434 (1983).

#185605 - $15.00 USD Received 19 Feb 2013; revised 20 Mar 2013; accepted 26 Mar 2013; published 2 Apr 2013

16. M. A. Model, A. K. Khitrin, and J. L. Blank, "Measurement of the absorption of concentrated dyes and their use for quantitative imaging of surface topography," J. Microsc. **231**(1), 156–167 (2008).
17. J. C. M. Antón, J. Alonso, J. A. G. Pedrero, and J. A. Quiroga, "Topographic optical profilometry by absorption in liquids," Opt. Express **20**(27), 28631–28640 (2012).
18. R. Barer and S. Joseph, "Refractometry of living cells," Q. J. Microsc. Sci. **95**, 399–423 (1954).
19. McCormick® Yellow Food Color.
20. J. Dai and M. P. Sheetz, "Membrane tether formation from blebbing cells," Biophys. J. **77**(6), 3363–3370 (1999).

1. Introduction

There has been an increasing effort to automate cell microscopy and to make it more quantitative. Measurements of the shape and volume of large collections of cells will enable the morphology of normal and abnormal samples to be better understood [1–5]. Accurate measurement of cell dimensions also convey information about cell growth rate, metabolism and osmotic pressure and protein concentration regulation [1,6,7]. Many recent demonstrations have relied on optical phase sensitive methods to measure cell shape and volume [8–13]. Unfortunately, the recovered optical phase is the product of the cell height and its local refractive index, which is frequently heterogeneous and may not be accurately known. The cell dimensions can be decoupled from the optical phase by taking consecutive measurements in buffers with different refractive index [8] or by optical tomography [14], but both are time consuming and not possible on cells in motion. Instead, we explore a method that measures cell height by quantifying the absorption of light passing through an absorbing dye that surrounds the cell. In this way, the optical properties of the cell do not need to be determined and have very little influence on the final measurement.

Measuring cell volume using an optical property of the surrounding fluid was first demonstrated in the context of flow cytometry [15]. In this case, fluorescent dye was added to the sample fluid, and a reduction in the observed fluorescence signal was measured when the cell traversed the laser detection region. The cell membrane is impermeable to the fluorescent dye, so the total number of fluorescence molecules in the laser detection region is reduced. The total cell volume, or the dye excluded volume, can then be determined if the geometry of the flow focus region is known or can be calibrated. A signal with higher contrast and lower noise can be obtained by measuring absorption instead of fluorescence. The surface profiles of adherent cells [16] and optical elements [17] have recently been measured by immersion in absorbing dyes. Here, we demonstrate the use of dye exclusion to measure height maps of live cells in suspension in a system called the dye exclusion microfluidic (DEM) microscope. Microfluidic channels are used to mechanically translate cells through the field of view and to precisely define the volume of the detection region. The DEM microscope combines the high measurement throughput of flow cytometry with the spatial resolution of microscopy. In addition, fluid flow enables the collection of images with and without each cell in the field of view, so that the transmission coefficients can be accurately evaluated.

2. Dye exclusion microscopy

The DEM microscope works on the principal that the absorption coefficient of a dye can be known extremely accurately. Figure 1(a) shows a diagram of the experimental setup. The cell is suspended in an absorbing dye inside a microfluidic channel with thickness (t). Light attenuates through the microfluidic channel according to Beer's law,

$$I_{cell}(x,y) = I_{ill}(x,y)e^{-\alpha(t-h(x,y))}, \tag{1}$$

where I_{cell} is the image intensity of the cell, and I_{ill} is the illumination intensity. For a known absorption coefficient (α), the height map (h) can be retrieved by solving Eq. (1),

$$h(x,y) = t + \log_e\left(I_{cell}(x,y)/I_{ill}(x,y)\right)/\alpha. \tag{2}$$

#185605 - $15.00 USD Received 19 Feb 2013; revised 20 Mar 2013; accepted 26 Mar 2013; published 2 Apr 2013

For an object that does not scatter light, a single measurement of I_{cell} would be enough to reconstruct an accurate height map. However, the measured intensity has contributions from light scattering as well as dye exclusion, which produces unwanted artifacts in the retrieved height maps.

We have minimized the contribution from scattering in two ways. Scattering losses arise from discontinuities in refractive index. For a cell suspended in a traditional buffer, such as phosphate buffer saline (PBS), the refractive index difference between the cell membrane (n = 1.41) and the buffer (n = 1.33) is the largest source of scattering loss. This loss can be reduced by using a buffer that has a refractive index that is matched to the average cell refractive index and constitutes the basis for cell refractometry [18]. For these experiments we have used a mixture of 36% glycerol, 24% bovine serum albumin, and 10% of a 10 × solution of PBS, in order to produce an isotonic buffer. This mixture has a refractive index of 1.41 at a wavelength of 589 nm, measured using an Abbe refractometer. Exact index matching is not critical, as scattering losses scale approximately proportional to Δn^2, so reducing Δn reduces scattering accordingly.

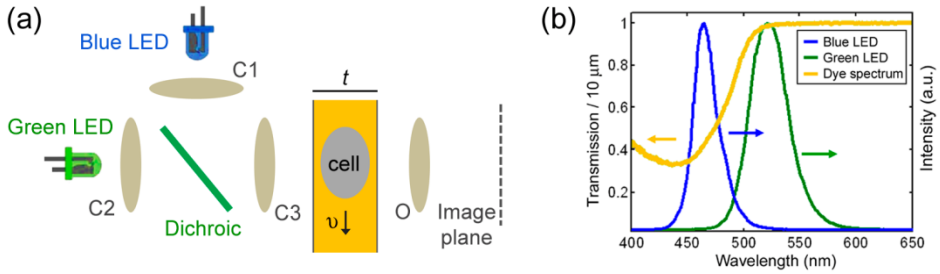

Fig. 1. The dye exclusion microfluidic (DEM) microscope. (a) Schematic of the experimental setup. A microfluidic channel is illuminated by a green and a blue LED combined with a dichroic mirror. C1, C2, and C3 are condenser lenses. The microfluidic channel is imaged using a 40 × , 0.75 NA Nikon Fluorite objective lens (O) onto a Pike 032c CCD camera from Allied Vision located at the image plane. (b) The transmission spectrum of the absorbing buffer and the emission spectrum of the green and blue LEDs.

Even if the refractive index of the buffer perfectly matches the cell average refractive index, internal structure inside the cell still contributes to scattering loss. To correct for internal scattering, we image the cell using two illumination colors, where one color is absorbed by the dye and the other is not. In this way, the image intensity for the absorbing color has contributions from both dye exclusion and scattering, while the image intensity for the non-absorbing color is solely due to scattering. For a cell that is weakly scattering and not absorbing, the contributions to the image intensity from scattering and absorption can be decoupled and written as,

$$I_{cell}(x,y,\lambda) = S(x,y,\lambda)e^{-\alpha_\lambda(t-h(x,y))}, \tag{3}$$

where the image intensity has been separated into its two components, S which is due to scattering loss, and the Beer's law term due to absorption. Scattering is a function of the wavelength (λ), so in order to obtain accurate scatter correction, two colors that are close in wavelength should be used.

In this work, we have chosen a yellow food dye composed of a mixture of Tartrazine and Allura Red in a solution of water and propylene glycol [19]. The transmission spectrum of the dye in the index matching buffer at a volume fraction of 0.25 is shown in Fig. 1(b), which shows an absorption peak centered at a wavelength of 440 nm. We use two LEDs for illumination, one centered at 465 nm (blue) and the other centered at 520 nm (green), whose spectra are also shown in Fig. 1b. The LEDs are operated in constant current mode and we use a color camera to separate the two color channels in a single exposure. The two LEDs

#185605 - $15.00 USD Received 19 Feb 2013; revised 20 Mar 2013; accepted 26 Mar 2013; published 2 Apr 2013

have a fractional wavelength difference of 12%. Data was collected from the camera in RAW format and we performed our own spectral demixing based on the cross-talk measured by illuminating the camera with the LED's individually. For these two LED's, the demixed images have close to zero cross-talk, but the broad response of the camera's Bayer filter would make it difficult to further reduce the fractional wavelength difference of the two colors.

3. Dye exclusion cytometry

Cells are suspended in the absorbing index-matching buffer and driven through a microfluidic channel using pressure driven flow. The microfluidic channel is 15 µm wide and measured to be 8 µm thick using a Dektak Profilometer, where the channel thickness defines the depth of the detection region. Figure 2(a) shows an image of an acute promyelocytic leukemia cell (HL60) under illumination by the blue and green LEDs. We measure the transmission coefficient of the green and blue LEDs inside the channel to be 0.995 and 0.418, respectively. From the measured transmission, the absorption coefficient in the green (α_g) is approximated as zero and the absorption coefficient in the blue (α_b) is calculated to be 0.109 µm^{-1}.

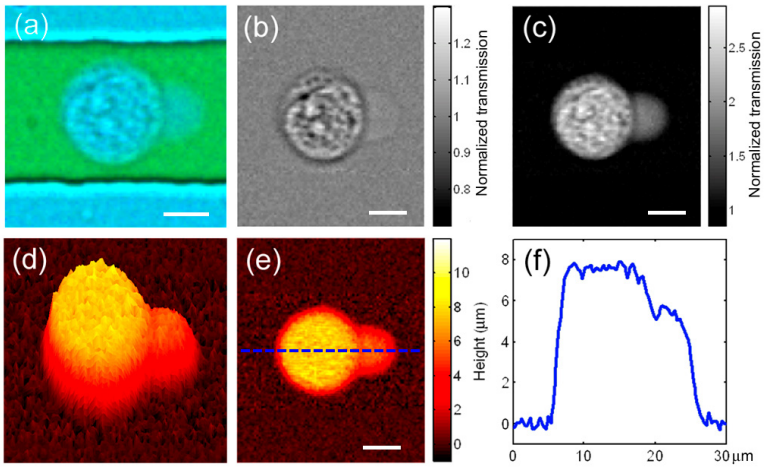

Fig. 2. Dye exclusion imaging of an HL60 cell. (a) Shows a composite image of the HL60 cell captured by the color camera under green and blue illumination. (b,c) Show normalized images of the green and blue channel, respectively. The scale bars show the normalized transmission values, with the background having a value of one. (d-f) Show the reconstructed height surface, height map, and a cross-section through the cell. All scale bars are 5 µm.

The microfluidic channel acts as a cell delivery system that enables extremely accurate transmission values to be measured because no mechanical motion other than fluid flow is needed to collect reference images. Normalized transmission (I_n) values are evaluated by dividing the image intensity with and without the cell for each of the two colors. From these two normalized images, the height map can be evaluated as,

$$h(x,y) = \frac{\log_e\left(I_n^{blue}(x,y)/I_n^{green}(x,y)\right)}{\alpha_B - \alpha_G}. \quad (4)$$

The only constants required for absolute height measurements are the absorption coefficients, as the channel height cancels due to the normalization. Figures 2(b)-2(c) show the normalized green and blue images, respectively, of the same cell shown in Fig. 2(a). The image from the green illumination shows scattering due to both the residual index mismatch between the cell and buffer and internal scattering. The normalized transmission values under green illumination range from 0.7 to 1.3. Problems can arise for cells with a much larger degree of

#185605 - $15.00 USD Received 19 Feb 2013; revised 20 Mar 2013; accepted 26 Mar 2013; published 2 Apr 2013

internal scattering, where the transmission values can locally approach zero. However, this was not an issue for all three cell types studied here when suspended in the index matching buffer. The image from the blue illumination exhibits both dye exclusion and scattering, but the net effect is that pixel values inside the cell are raised above the background, as shown in Fig. 2(c).

Using both normalized images, the height map is computed and shown in Figs. 2(d)-2(f). The internal scattering is effectively removed and the top of the cell has a flat profile due to the roof of the microfluidic channel. One interesting feature of this cell is the bleb that appears on its downstream (right) side. A bleb is a region where the cell membrane has detached from the cytoskeleton and is inflated due to the cell's Laplace pressure [20]. Because the bleb is a small volume of cytoplasm that does not contain any major cell organelles, it scatters very little and is almost invisible under green illumination. The bleb does however exclude the absorbing dye and consequently is easily visible under blue illumination.

As seen in Figs. 2(d)-2(f), the height map background is flat and has zero mean. The standard deviation of the background is 300 nm inside the channel and 200 nm outside the channel. There are no artifacts due to halo patterns and shade-off, as in the common-path quantitative phase imaging method, or enhanced low frequency noise, as in the transport of intensity equation phase imaging method. The height roughness is due to photon shot noise and could be considerably reduced by temporal or spatial averaging. For the measurements shown in this work, the average flow velocity (υ) is 5 mm/s, exposure time is 150 μs and the camera collects 300 frames per second.

Microfluidic cell delivery enables automated collection of large numbers of cells. Figure 3 shows image sets of three leukemia cell lines, acute lymphoblastic (Molt4), acute promyelocytic (HL60), and chronic myelogenous (K562). A threshold is applied to the reconstructed height maps to define the cell region. The volume of the cell can then be calculated by integrating all the thickness values inside the cell and multiplying by the pixel area. Figure 3 shows histograms of cell volumes for all three cell lines. The Molt4 cells are the smallest, with a mean (m) of 718 fL and a standard deviation (σ) of 232 fL, followed by the HL60 cells with an m of 1110 fL and a σ of 466 fL, and the K562 cells are the largest, with an m of 1480 fL and a σ of 661 fL. We have verified these values using a Coulter counter (Beckman Coulter, Multisizer 3) on the HL60 cells. The peak value of the volume histogram occurred at 818 fL for the Multisizer 3 and occurs at 831 fL in our histogram. The mean as measured by our system is biased to a larger measured volume due to a higher coincidence rate than the Multisizer 3, but the central peak is located at the same location and has a similar shape. At the current flow velocity and frame rate, each cell can be measured multiple times before it leaves the field-of-view. The coefficient of variation of the measured volume was 0.0038 for different images of the same cell, corresponding to a reproducibility of better than one part in 250. However, there is only a small rotation of the cell in between frames, so this does not completely take into account the total possible variance due to a random orientation.

#185605 - $15.00 USD Received 19 Feb 2013; revised 20 Mar 2013; accepted 26 Mar 2013; published 2 Apr 2013

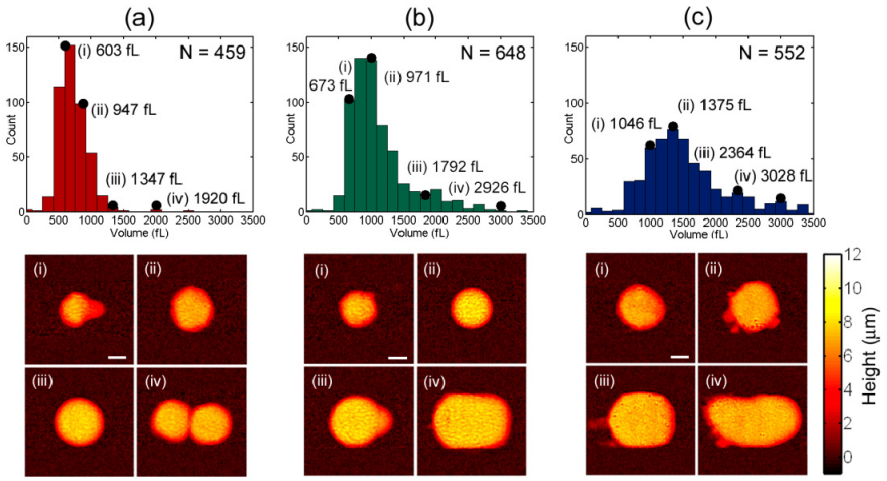

Fig. 3. Height map image sets of three leukemia cell lines. For each image set a volume histogram is shown and four representative height maps are displayed below. (a) Image set of Molt4 cells. (b) Image set of HL60 cells. (c) Image set of K562 cells. N is the number of cells in each histogram. All scale bars are 5 µm.

Figure 3 shows four sample images of each cell line, taken from the much larger image set. As can be seen in Fig. 3(a), the Molt4 cells have a symmetric volume distribution, where the few cells that are significantly larger than average are aggregates. The HL60 and K562 cells, however, shown in Figs. 3(b)-3(c), have a more asymmetric distribution due to the presence of cells that have volumes as large as 3000 fL. It is common for the K562 cells to have membrane protrusions, as seen in the second, third, and fourth panels, but these are not captured in the histogram plots. By capturing the thickness maps of all analyzed cells, complex image metrics can be evaluated to study and discriminate cells beyond what is possible with just volume histograms. Analysis of the height maps also enables the measurement of subcellular features, such as blebs and protrusions. We also believe that this imaging method will be useful for studies on three-dimensional cellular deformability as a function of hydrodynamic shear.

4. Conclusion

We have demonstrated an optical method called the DEM microscope that measures height maps of cells in suspension. The DEM microscope uses microfluidics to precisely define a confined sample volume and to transport cells through this region. We have corrected errors that arise due to scattering artifacts using a refractive index matching buffer and a two color correction scheme. The results compare closely to those obtained using a Coulter counter on the position of the peak value of a volume histogram of HL60 cells. In addition to accurate volume measurements, the spatial resolution provided by the DEM microscope will enable characterization of small extracellular morphological features and also simultaneous measurement of cell protein concentrations using fluorescence. By measuring absorption in a well characterized dye, the DEM microscope is able to accurately measure cell geometry independent of the cells optical properties.

Acknowledgments

Ethan Schonbrun would like to thank the Rowland Junior Fellows program which supported this work.

#185605 - $15.00 USD Received 19 Feb 2013; revised 20 Mar 2013; accepted 26 Mar 2013; published 2 Apr 2013